Average Age-of-Information Minimization in Aerial IRS-Assisted Data Delivery

Wenwen Jiang, *Graduate Student Member, IEEE*, Bo Ai, *Fellow, IEEE*, Mushu Li, *Member, IEEE*, Wen Wu, *Senior Member, IEEE*, and Xuemin Shen, *Fellow, IEEE*

Abstract—Aerial intelligent reconfigurable surface (IRS) is a promising technology to enhance channel quality in data delivery. In this article, we study an aerial IRS deployment problem to enable timely and reliable data delivery in a remote Internet of Things (IoT) scenario, in which an IRS mounted on an unmanned aerial vehicle (UAV) is adopted as a mobile relay to assist devices in uploading data to the base station (BS). The objective is to minimize the average Age of Information (AoI) of the data received by the BS over time by jointly determining the aerial IRS deployment position and phase shift, transmit power of devices, and data uploading time. Under the requirements of peak AoI (PAoI) and communication reliability, we formulate an average AoI minimization problem. Since the nonlinear relations among optimization variables make the formulated problem nonconvex and intractable to solve, we propose a block coordinate descent (BCD)-based iterative algorithm which decomposes the formulated problem into several subproblems. The variables are optimized in each subproblem individually in an alternately iterative manner to attain a near-optimal solution. Simulation results demonstrate the superiority of the proposed algorithm in improving the information freshness compared with the benchmark schemes.

Index Terms—Age of Information (AoI), intelligent reconfigurable surface (IRS), joint optimization, unmanned aerial vehicle (UAV), wireless data delivery.

Wenwen Jiang and Bo Ai are with the State Key Laboratory of Rail Traffic Control and Safety, Beijing Jiaotong University, Beijing 100044, China (e-mail: wenwenjiang@bjtu.edu.cn; boai@bjtu.edu.cn).

Mushu Li is with the Department of Electrical, Computer, and Biomedical Engineering, Toronto Metropolitan University, Toronto, ON M5B 2K3, Canada (e-mail: mushu.li@ieee.org).

Wen Wu is with the Frontier Research Center, Peng Cheng Laboratory, Shenzhen 518055, China (e-mail: wuw02@pcl.ac.cn).

Xuemin Shen is with the Department of Electrical and Computer Engineering, University of Waterloo, Waterloo, ON N2L 3G1, Canada (e-mail: sshen@uwaterloo.ca).

Digital Object Identifier 10.1109/JIOT.2023.3264618

I. Introduction

THE COMMERCIALIZATION of the fifth-generation (5G) networks has fostered a large number of time-critical applications [1], such as intelligent transportation systems [2] and remote environmental monitoring [3]. In these applications, the information freshness of data is essential for monitoring network status accurately or making decisions timely, especially in safety-related applications [4]. The transmission of outdated information may result in the waste of communication resources and even serious damage. To properly quantify the freshness of information, the metric *Age of Information* (AoI) [5], [6], [7] can be a key performance indicator (KPI) for time-critical applications. AoI is defined as the time elapsed since its most recent status update was generated [5]. Different from other metrics, such as end-to-end transmission delay, AoI is a metric that dynamically evolves with time, which characterizes the evolution of information freshness over time [6]. The maximum value of AoI before a new information update arrived at the receiver is defined as *peak AoI* (PAoI) [7]. The maximum value of AoI can be limited by the PAoI requirement.

Information freshness is essential for time-critical applications. However, it is challenging for remote Internet of Things (IoT) [8] devices to keep the freshness of information contained in the transmission data. This is because it is difficult for devices distributed in the suburbs to reliably transmit data to the receiver over a long distance, especially for energy-limited devices or blocked propagation environment. Therefore, delivering data in a timely and reliable manner is critical to improving the information freshness of the transmission data in time-critical applications. To this end, unmanned aerial vehicles (UAVs) [9] and intelligent reconfigurable surface (IRS) [10], [11], [12] can be considered promising technologies to enhance the communication quality. The aerial IRS [13], i.e., the IRS mounted on the high-altitude platforms [14] or UAVs [15], is regarded as a promising solution to improve the information freshness [16] in time-critical applications.

UAVs have been deployed widely to provide on-demand services as multifarious flying platforms [17], [18], [19]. Due to the high flight altitude and flexible deployment, UAVs can be dispatched to assist communication for devices with limited energy capacity or maximum transmit power by establishing Line-of-Sight (LoS) links [20]. However, the endurance time is a bottleneck for UAV-assisted communications. UAV trajectory

is thus required to be well-designed to enlarge the endurance time. In addition, UAV-assisted relay transmission introduces additional intermediate delay [21] and the UAV needs to bear additional processing and transmission power consumption. While for IRS, as one of the new emerging revolutionary technologies for 6G [22], [23], [24], it can be used as the controllable passive relay for improving the channel quality. IRS is a planar metasurface that consists of a large number of low-cost and passive reflecting elements, while each element can independently shift the phase of the electromagnetic waves impinging on itself with minimal power consumption. Despite these advantages, the deployment of terrestrial IRS is highly restricted by the network environment and scenarios [24]. Once the terrestrial IRS is deployed, its position generally cannot be moved, which limits the coverage that the IRS can provide and thus limits the potential channel enhancement.

Fortunately, the aerial IRS can address the limitations of UAV and terrestrial IRS. The aerial IRS is more likely to establish strong LoS links with the ground devices due to the higher altitudes of the UAV. Furthermore, aerial IRS can adjust its positions dynamically according to the changes in the network environment and thus can maintain persistent reliable links between transceivers. However, there are still several critical issues that need to be solved. First, the aerial IRS deployment, which determines the quality of the established channel, needs to be well-designed to improve the information freshness and increase the UAV flying endurance. Second, multiple types of resources, i.e., communication, energy, and time resources, should be jointly allocated to enable efficient aerial IRS. Finally, it is challenging to analyze the AoI evolution, derive its expressions under different system frameworks, and deal with the difficulties of joint optimization, such as variable coupling, nonconvex constraints, etc.

In this article, we investigate an average AoI minimization problem in a remote IoT scenario, where an aerial IRS is adopted as a passive relay to assist in delivering the data generated by devices with limited energy budgets to a faraway base station (BS). In this scenario, we first analyze the evolution of AoI over time and derive the expression of PAoI. To improve the information freshness of data received by the BS, we formulate an average AoI minimization problem under the requirements of PAoI and communication reliability by jointly optimizing the aerial IRS deployment and phase shift, transmit power of devices, and data uploading time. Due to the coupling among these optimization variables and the nonconvexity of constraints, it is intractable to solve the formulated problem directly. To deal with this issue, we develop an iterative algorithm based on the block coordinate descent (BCD) method [25] to solve the nonconvex average AoI minimization problem. Simulation results demonstrate the effectiveness of the algorithm developed in this article in improving the information freshness. The main contributions of this article are summarized as follows.

1) We propose a BCD-based iterative algorithm, which can provide a flexible aerial IRS deployment and resource management solution to improve the information freshness in aerial IRS-assisted data delivery.

2) Under the coupling nature of AoI in time, we decompose the nonconvex AoI minimization problem and develop an iterative algorithm to solve it in an alternating manner. This provides ideas to cope with the complex nonconvex problems with coupling relations among variables.

3) The BCD-based iterative algorithm can achieve a near-optimal solution with limited time complexity. Extensive simulations are provided to demonstrate that the proposed solution performs better than the fixed aerial IRS deployment (FIRS) and the active relay (AcRelay), i.e., UAV.

The remainder of this article is organized as follows. Section II reviews the related work. Section III presents the system model and formulates the average AoI minimization problem. An iterative algorithm is developed based on the BCD method in Section IV. Simulation results are presented in Section V. Finally, conclusions are drawn in Section VI.

Notations: Scalars, column vectors, and matrices are written in italic, boldfaced lowercase, and uppercase letters, respectively, e.g., a, $\boldsymbol{a}$, and $\boldsymbol{A}$. The superscripts $(\cdot)^{\mathrm{H}}$ and $(\cdot)^{\mathrm{T}}$ indicate the Hermitian transpose and the transpose, respectively. The operator $\|\cdot\|_2$ represents the ℓ_2-norm of the vector. In addition, the space of M-dimensional real vector and complex vector are denoted by $\mathbb{R}^M$ and $\mathbb{C}^M$, respectively. $\mathbb{C}^{M \times M}$ represents the space of $M \times M$ dimensional complex space. The logarithm with base 2 is denoted by $\log_2(\cdot)$. $\otimes$ represents the Kronecker product. Given set $\mathcal{K} \triangleq \{1, \ldots, K\}$, $\tilde{\mathcal{K}} \triangleq \mathcal{K} \backslash \{K\}$ represents the set of elements in $\mathcal{K}$ except K.

II. RELATED WORK

A. UAV-Assisted Communications

UAVs have been used as flying communication platforms in military and commercial applications to enable energy-efficient network design [17], [18], [19], assist in timely data collection [26], [27], or enlarge communication coverage [28]. These studies focus on the optimization related to network efficiency and UAV endurance. Among the existing research work on UAV-assisted communications, there are also some efforts to pay attention to the optimization of information freshness. An AoI-based UAV trajectory planning problem for data collection was investigated in [29]. This work minimized the AoI of collected IoT data by designing the UAV trajectory considering uncertain data arrival patterns. The authors investigated an average PAoI minimization problem for a source-destination pair with the assistance of a UAV as a mobile relay [30]. Jiang et al. [31] studied the average PAoI minimization problem in a UAV-assisted wireless sensor network, where the UAV assists in data collection and forwarding as a mobile relay. Zhang et al. [32] addressed an AoI minimization problem in a UAV-assisted cellular network by jointly optimizing service time, UAV trajectory, and task scheduling. Wu et al. [33] proposed an AI-based framework for data collection in wireless sensor networks, where the UAV trajectory is designed to minimize the maximum AoI and the average AoI.

B. IRS-Enabled UAV Communications

The potential topics and solutions on combining UAV and IRS have been discussed in [24]. Existing studies on

IRS-enabled UAV communication can be divided into two types: 1) terrestrial IRS [34], [35] and 2) aerial IRS [36]. Al-Hilo et al. [34] studied a UAV-assisted data collection problem from multiple devices with the time constraint. A terrestrial IRS in [34] was deployed to improve both the connectivity and energy efficiency of the UAV. Mu et al. [35] proposed a new transmission framework for maximization of the sum rate of networks, where multiple UAV-mounted BSs employ nonorthogonal multiple access (NOMA) to serve multiple groups of ground users with the aid of an IRS. Khalili et al. [36] investigated a total transmit power minimization problem by jointly optimizing each UAV trajectory/velocity, IRS phase shift, subcarrier allocations, and active beamformers at each BS. This work revealed that the transmit power can be reduced by 6 dBm by deploying aerial IRSs while maintaining a similar Quality of Service (QoS). The research on AoI-oriented optimization with aerial IRS assistance is still in its infancy.

C. AoI Optimization With Aerial IRS Assistance

Although the aerial IRS is expected to be an efficient solution to improve the information freshness and communication quality, there is little research on AoI optimization with aerial IRS assistance. Samir et al. [21] investigated an expected sum AoI minimization problem by jointly optimizing the altitude of the UAV, the communication schedule, and IRS phases shift in an aerial IRS-assisted IoT network. They developed an approach to solve the joint optimization problem based on proximal policy optimization algorithm. This work is the first study on AoI optimization via the assistance of aerial IRS. Lyu et al. [37] studied a packet scheduling problem in a terrestrial wireless network assisted by an aerial IRS. They jointly optimize the UAV trajectory, passive and active beamforming, and scheduling scheme based on successive convex approximation (SCA) algorithm to minimize the weighted sum of AoI of all ground users.

These works provide insights into applying the aerial IRS in time-critical applications to satisfy the AoI requirements. In this article, we propose an offline design for dynamic deployment of aerial IRS based on convex programming to improve information freshness. Different from assuming that the communication is completed within a time slot, we calculate the exact data uploading time according to the data size and transmission rate. As such, we can characterize the AoI evolution more accurately to study the impact of communication network parameters on AoI.

III. SYSTEM MODEL AND PROBLEM FORMULATION

A. Scenario Model

We consider an aerial IRS-assisted remote IoT communication scenario, as shown in Fig. 1, wherein there are one aerial IRS, one BS, and K ground IoT devices. In this scenario, the devices with limited energy capacity need to upload the data timely to the BS for further processing. Due to the long distance, communication links between the devices and the BS cannot be established directly. Thus, an aerial IRS is employed as a mobile and passive relay to assist in the data delivery for
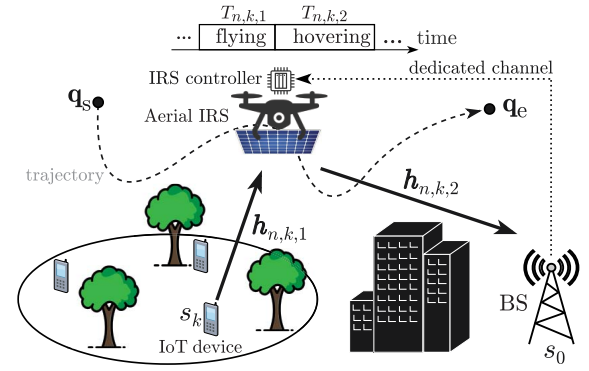
Fig. 1. System model of an aerial IRS-assisted wireless network.

improving communication quality and information freshness. The service sequence for devices is preassigned. To ensure the stability of the established channel, the deployment position of the aerial IRS is considered unchanged [21] when assisting one device in uploading. The BS and K devices are each equipped with an omnidirectional antenna, while the aerial IRS is fitted with a uniform planar array (UPA) of M reflective elements. The phase shift of each IRS reflective element is controlled by the IRS controller mounted on the UAV based on the results provided by the BS. In addition, we denote the position of the BS by $s_0 = (x_0, y_0) \in \mathbb{R}^2$, and the position of the kth device by $s_k = (x_k, y_k) \in \mathbb{R}^2 \ \forall k \in \mathcal{K} \triangleq \{1, \ldots, K\}$. The flight altitude of the aerial IRS is fixed as h. The starting position and end position of the aerial IRS are denoted by $\mathbf{q}_s = (x_s, y_s) \in \mathbb{R}^2$ and $\mathbf{q}_e = (x_e, y_e) \in \mathbb{R}^2$, respectively.

We define a time frame as the total time for the aerial IRS to assist K devices to upload status packets to the BS. At the end of a time frame, K data packets are uploaded. Since the status information of the device changes over time, the packet delivery process needs to be executed repeatedly to ensure that the BS can receive the status information as fresh as possible. This system is considered to work on N time frames.

In this scenario, the aerial IRS can flexibly adjust its deployment positions toward devices in different positions. Specifically, the aerial IRS first departs from starting position $\mathbf{q}_s$ and flies to a suitable position to assist the first device to upload its packet. The position remains unchanged when the aerial IRS assists one device in uploading to maintain stability of the established communication link. After that, the aerial IRS moves to the next position to assist with uploading for another device. Until the communication tasks within N time frames are completed, the aerial IRS flies to the end position $\mathbf{q}_e$ directly. The aerial IRS is required to assist each device in uploading one packet within a time frame. Thus, the nth time frame, which is denoted by T_n, can be divided into K service time segments, where T_n can be mathematically expressed by

$$T_n = \sum_{k=1}^{K} T_{n,k} \ \forall n \in \mathcal{N} \triangleq \{1, \ldots, N\} \qquad (1)$$

where $T_{n,k}$ is the service time for the kth device in the nth time frame, further, it contains two parts

$$T_{n,k} = T_{n,k,1} + T_{n,k,2} \ \forall n \in \mathcal{N}, k \in \mathcal{K} \qquad (2)$$
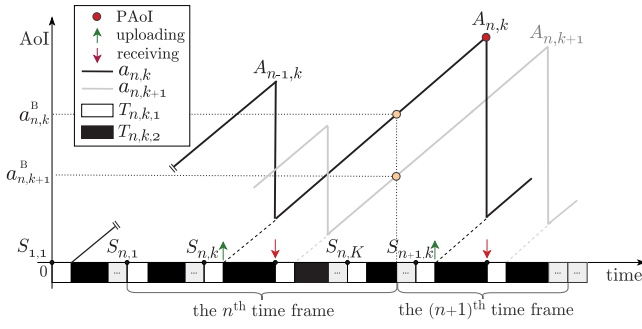
Fig. 2.   Example of AoI evolving over time frames.

where $T_{n,k,1} \in \mathbb{R}$ is the flying time used to deploy the aerial IRS, and $T_{n,k,2} \in \mathbb{R}$ is the hovering time used to upload the status packet.

We denote the starting moment of the nth time frame T_n and the starting moment of the service time $T_{n,k}$ by S_n and $S_{n,k}$, respectively. As shown in Fig. 2, the relationship between S_n and $S_{n,k}$ can be expressed as

$$S_{n,1} = S_n \ \forall n \in \mathcal{N} \tag{3a}$$

$$S_{n,k} = S_n + \sum_{i=1}^{k-1} T_{n,i} \ \forall n \in \mathcal{N}, k \in \mathcal{K}. \tag{3b}$$

Since the IRS is mounted on the UAV, the internal distance between the UAV and the IRS can be negligible compared to the long communication distances. The positions of the UAV and the IRS can be considered the same. The aerial IRS trajectory can be approximated by a series of discrete positions. Specifically, the position of the aerial IRS at the time instant $S_{n,k} + T_{n,k,1}$ is denoted by $\mathbf{q}_{n,k} = (x_{n,k}, y_{n,k}) \in \mathbb{R}^2$. The variable $\mathbf{q}_{n,k}$ remains unchanged for $T_{n,k,2}$ period during the process of uploading.

Due to the mechanical and regulatory limitations, the UAV has a flight speed limit which is denoted by $v_{\max}$. The distance constraints over consecutive positions due to the flight speed limit can be modeled by

$$\|\mathbf{q}_{1,1} - \mathbf{q}_s\|_2 \le T_{1,1,1} v_{\max} \tag{4a}$$

$$\|\mathbf{q}_{n,k+1} - \mathbf{q}_{n,k}\|_2 \le T_{n,k+1,1} v_{\max} \ \forall n \in \mathcal{N}, k \in \bar{\mathcal{K}} \tag{4b}$$

$$\|\mathbf{q}_{n+1,1} - \mathbf{q}_{n,K}\|_2 \le T_{n+1,1,1} v_{\max} \ \forall n \in \bar{\mathcal{N}}, k \in \mathcal{K} \tag{4c}$$

$$\|\mathbf{q}_e - \mathbf{q}_{N,K}\|_2 \le (T_{\max} - S_N - T_N) v_{\max} \ \forall n \in \bar{\mathcal{N}}, k \in \mathcal{K} \tag{4d}$$

where $\bar{\mathcal{K}} \triangleq \mathcal{K} \backslash \{K\}$ represents the set of devices other than K, and $\bar{\mathcal{N}} \triangleq \mathcal{N} \backslash \{N\}$ is defined similarly. In (4d), $T_{\max}$ is the maximum battery life of the UAV. Equations (4a) and (4d) require that the aerial IRS should depart from the starting position $\mathbf{q}_s$, and to the end position $\mathbf{q}_e$ when all the tasks within N time frames are completed. Equations (4b) and (4c) are the constraints between the adjacent devices and time frames, respectively.

B. Communication Model

For the aerial IRS with M reflective elements, we define the diagonal phase-shift of the aerial IRS for the kth device in the nth time frame as $\Theta_{n,k} =$

$\mathrm{diag}\{e^{j\theta_{n,k}[1]}, \ldots, e^{j\theta_{n,k}[m]}, \ldots, e^{j\theta_{n,k}[M]}\} \in \mathbb{C}^{M \times M}$ with $\theta_{n,k}[m] \in [0, 2\pi), m \in \mathcal{M} \triangleq \{1, \ldots, M\}$. $\theta_{n,k}[m]$ represents the phase shift of the mth element for the kth device in the nth time frame. Although the direct links between the BS and devices can not be established, there exist links assisted by the aerial IRS. Thanks to the high-probability LoS links establishment of the UAV [20], the link from devices to the aerial IRS (D-R) and the link from the aerial IRS to the BS (R-B) can both be modeled by the Rician fading channel with a dominant LoS model [21], [38], [39]. Therefore, the channel gain of the D-R link denoted by $\boldsymbol{h}_{n,k,1} \in \mathbb{C}^{M \times 1}$ is defined by

$$\boldsymbol{h}_{n,k,1} = \sqrt{\rho d_{n,k,1}^{-\alpha}} \beta \bar{\boldsymbol{h}}_{n,k,1}(\phi_{n,k}^r, \eta_{n,k}^r) \ \forall n \in \mathcal{N}, k \in \mathcal{K} \tag{5}$$

where $\sqrt{\rho d_{n,k,1}^{-\alpha}}$ represents the path loss coefficient, ρ is the average path loss at a reference distance of one meter, α represents the path loss exponent, and $\beta \triangleq \sqrt{[\kappa/(\kappa+1)]}$ where κ is the Rician factor. $d_{n,k,1} \triangleq \sqrt{\|\mathbf{q}_{n,k} - \boldsymbol{s}_k\|_2^2 + h^2}$ is the distance between the aerial IRS and the kth device in the nth time frame. $\phi_{n,k}^r$ and $\eta_{n,k}^r$ are the azimuth angle and the elevation steering angle from the kth device to the aerial IRS, respectively.

The indices along the X and Y axes for the IRS elements are denoted by $0 \le m_x \le M_x$ and $0 \le m_y \le M_y$, respectively, where $M = M_x M_y$. The mth reflective element is denoted as $m = m_y(m_x - 1) + m_y$. Then, we set $u_{n,k}^r \triangleq \sin(\phi_{n,k}^r) \cos(\eta_{n,k}^r)$, and $w_{n,k}^r \triangleq \sin(\phi_{n,k}^r) \sin(\eta_{n,k}^r)$, the steering vector $\bar{\boldsymbol{h}}_{n,k,1}(\phi_{n,k}^r, \eta_{n,k}^r)$ is given by

$$
\begin{aligned}
\bar{\boldsymbol{h}}_{n,k,1}(\phi_{n,k}^r, \eta_{n,k}^r) &= \left(1, \ldots, e^{-j\frac{2\pi d}{\lambda}(M_x-1)\sin(\phi_{n,k}^r)\cos(\eta_{n,k}^r)}\right) \\
&\otimes \left(1, \ldots, e^{-j\frac{2\pi d}{\lambda}(M_y-1)\sin(\phi_{n,k}^r)\sin(\eta_{n,k}^r)}\right) \\
&= \left[1, \ldots, e^{-j\frac{2\pi d}{\lambda}\left(m_x u_{n,k}^r + m_y w_{n,k}^r\right)}, \ldots, \right. \\
&\quad \left. e^{-j\frac{2\pi d}{\lambda}\left((M_x-1)u_{n,k}^r + (M_y-1)w_{n,k}^r\right)}\right]^{\mathrm{T}}
\end{aligned} \tag{6}
$$

where λ and d represent the carrier wavelength and the spacing between the IRS elements, respectively. $\eta_{n,k}^r$ and $\phi_{n,k}^r$ can be calculated as $\eta_{n,k}^r = \arctan((\|\mathbf{q}_{n,k} - \boldsymbol{s}_k\|_2)/h)$, $\phi_{n,k}^r = \arctan([\bar{y}_k - y_{n,k}]/[\bar{x}_k - x_{n,k}]) - \pi \min(\mathrm{sgn}(\bar{x}_k - x_{n,k}), 0) \ \forall n \in \mathcal{N}, k \in \mathcal{K}$.[1]

Similarly, the channel gain of the R-B link $\boldsymbol{h}_{n,k,2} \in \mathbb{C}^{M \times 1}$ is given by

$$\boldsymbol{h}_{n,k,2} = \sqrt{\rho d_{n,k,2}^{-\alpha}} \beta \bar{\boldsymbol{h}}_{n,k,2}(\phi_{n,k}^t, \eta_{n,k}^t) \ \forall n \in \mathcal{N}, k \in \mathcal{K} \tag{7}$$

where $\phi_{n,k}^t$ and $\eta_{n,k}^t$ are the azimuth angle and the elevation steering angle from the aerial IRS to the BS, respectively. In (7), $d_{n,k,2} \triangleq \sqrt{\|\mathbf{q}_{n,k} - \boldsymbol{s}_0\|_2^2 + h^2}$ is the distance between the aerial IRS and the BS in the nth time frame. $\bar{\boldsymbol{h}}_{n,k,2}(\phi_{n,k}^t, \eta_{n,k}^t)$ is the steering vector in $\boldsymbol{h}_{n,k,2}$, where $u_{n,k}^t \triangleq \sin(\phi_{n,k}^t) \cos(\eta_{n,k}^t)$,

---

[1]The function sgn represents the sign function used to extract the sign of a real number, which is defined as $\mathrm{sgn}(x) = \begin{cases} 1, & x > 0, \\ 0, & x = 0, \\ -1, & x < 0, \end{cases}$ for any real number x.

and $w_{n,k}^t \triangleq \sin(\phi_{n,k}^t)\sin(\eta_{n,k}^t)$. The calculation of $\bar{h}_{n,k,2}$ which is similar to $\bar{h}_{n,k,1}$ is omitted here for brevity. Therefore, the overall channel gain between the kth device and the BS via the aerial IRS is expressed as

$$
\begin{aligned}
H_{n,k} &= h_{n,k,2}^H \Theta_{n,k} h_{n,k,1} \\
&= \rho \beta^2 \sqrt{d_{n,k,1}^{-\alpha} d_{n,k,2}^{-\alpha}} \sum_{m=1}^{M} e^{j(\theta_{n,k}[m] + \psi_{n,k,m} - \varphi_{n,k,m})}
\end{aligned} \tag{8}
$$

for all $n \in \mathcal{N}, k \in \mathcal{K}, m \in \mathcal{M}$, where $\psi_{n,k,m} \triangleq [(-2\pi d)/\lambda](m_x u_{n,k}^r + m_y w_{n,k}^r)$, and $\varphi_{n,k,m} \triangleq [(-2\pi d)/\lambda](m_x u_{n,k}^t + m_y w_{n,k}^t)$.

Due to the limited radio frequency output power, each device has a maximum power $P_{\max}$. In addition, each device needs to upload N status packets within a given energy budget $E_{\max}$. The transmit power of the kth device in the nth time frame is denoted by $p_{n,k}$, which is subject to

$$
0 \le p_{n,k} \le P_{\max} \quad \forall n \in \mathcal{N}, k \in \mathcal{K} \tag{9a}
$$

$$
\sum_{n=1}^{N} p_{n,k} T_{n,k,2} \le E_{\max} \quad \forall k \in \mathcal{K}. \tag{9b}
$$

Then, the received signal-to-noise ratio (SNR) at the BS can be expressed as

$$
\gamma_{n,k} = \frac{p_{n,k} |H_{n,k}|^2}{\sigma^2} \quad \forall n \in \mathcal{N}, k \in \mathcal{K} \tag{10}
$$

where σ^2 is the variance of additive white Gaussian noise (AWGN) power at the BS. We assume that the perfect channel state information (CSI) can be obtained by the existing channel estimation methods [40]. The communication bandwidth is denoted by B. Thus, according to the Shannon capacity, the achievable rate for the kth target in the nth time frame $R_{n,k}$ bps/Hz is given by

$$
R_{n,k} = B \log_2(1 + \gamma_{n,k}) \quad \forall n \in \mathcal{N}, k \in \mathcal{K}. \tag{11}
$$

To guarantee the communication quality, the achievable throughput for the kth target in the nth time frame is required to be no less than the packet size D_s for ensuring the reliable transmission, i.e.,

$$
B T_{n,k,2} \log_2(1 + \gamma_{n,k}) \ge D_s \quad \forall n \in \mathcal{N}, k \in \mathcal{K}. \tag{12}
$$

C. Age of Information Model

The queue length at each device is set to one, which means that the newly arrived packet must replace the older packet. The just-in-time transmission policy [5] is adopted in this article. This policy requires that once the device receives the message that requests device uploading from the UAV, it can upload the latest status packet immediately. In this article, the AoI characterizes the time evolution from the packet generation to the reception by the BS, as shown in Fig. 2. Specifically, we denote the AoI value for the kth device in the nth time frame by $a_{n,k}$, which starts from the time instant $S_{n,k} + T_{n,k,1}$. The AoI value $a_{n,k}$ keeps increasing linearly until a new status packet is received by the BS in the $(n+1)$th time frame, and the AoI of the nth status packet for the kth device will reach its peak, denoted by $A_{n,k}$. After that, the AoI in the

$(n+1)$th time frame which is denoted by $a_{n+1,k}$ will drop to the AoI value of the latest received status packet, i.e., $T_{(n+1),k,2}$. Then, before a new status packet is received in the next time frame, the AoI still grows linearly over time. Thus, the AoI evolution over time for the kth device within adjacent time frames is expressed as

$$
a_{n+1,k} = \begin{cases} a_{n,k}^B + (t - S_{n+1}), & S_{n+1} \le t < S_{n+1,k} + T_{n+1,k} \\ t - (S_{n+1,k} + T_{n+1,k,1}), & S_{n+1,k} + T_{n+1,k} \le t < S_{n+2} \end{cases} \tag{13}
$$

for all $n \in \bar{\mathcal{N}}$ and $k \in \mathcal{K}$, where $a_{n,k}^B$ is the AoI value observed at the BS for the kth device when the nth time frame ends, which is given by

$$
a_{n,k}^B = \sum_{i=k}^{K} T_{n,i} - T_{n,k,1} \quad \forall n \in \mathcal{N}, k \in \mathcal{K}. \tag{14}
$$

We assume that the system has not received any status packet from devices before running. The AoI evolution for the kth device in the first time frame is given by

$$
a_{1,k} = \begin{cases} 0, & S_1 \le t < S_{1,k} + T_{1,k,1} \\ t - (S_{1,k} + T_{1,k,1}), & S_{1,k} + T_{1,k,1} \le t < S_2 \end{cases} \tag{15}
$$

for all $k \in \mathcal{K}$. It is worth mentioning that there is no peak in the first time frame due to the initial state of the system.

To improve the freshness of the status packets received by the BS, we aim to minimize the average AoI (AO) observed at the BS for all devices over N time frames. Time discretization is adopted to avoid the difficulty of integration in finding the average AoI. Thus, AO is expressed as

$$
\text{AO} = \frac{1}{NK} \sum_{n=1}^{N} \sum_{k=1}^{K} a_{n,k}^B \quad \forall n \in \mathcal{N}, k \in \mathcal{K}. \tag{16}
$$

In addition, the PAoI of the nth status packet for the kth device $A_{n,k}$ is given by

$$
A_{n,k} = S_{n+1,k} + T_{n+1,k} - (S_{n,k} + T_{n,k,1}) \tag{17a}
$$

$$
= \sum_{i=k}^{K} T_{n,i} + \sum_{i=1}^{k} T_{n+1,i} - T_{n,k,1} \quad \forall n \in \bar{\mathcal{N}}, k \in \mathcal{K}. \tag{17b}
$$

To ensure the QoS, we require that the PAoI for each device should be no larger than an upper limit A_{th}, i.e.,

$$
A_{n,k} \le A_{th} \quad \forall n \in \bar{\mathcal{N}}, k \in \mathcal{K}. \tag{18}
$$

D. Problem Formulation

The AoI evolution process indicates that AoI is coupled in service time, i.e., aerial IRS flight time and data uploading time of devices, which is indirectly determined by the transmit power of devices, the aerial IRS deployment, and the phase-shift design. To improve the information freshness, we aim to minimize the average AoI of all status packets received by the BS. Thus, the joint optimization problem is formulated as

$$
(\text{P1}) \quad \min_{\mathbf{P}, \mathbf{T}, \mathbf{Q}, \Theta} \text{AO} \tag{19a}
$$

$$
\text{s.t.} \quad 0 \le \theta_{n,k}[m] < 2\pi \quad \forall n \in \mathcal{N}, k \in \mathcal{K}, m \in \mathcal{M} \tag{19b}
$$

$$
(4), (9a), (9b), (12), (18)
$$

where $\mathbf{P} = \{p_{n,k} \; \forall n, k\}$, $\mathbf{T} = \{T_{n,k,1}, T_{n,k,2} \; \forall n, k\}$, $\mathbf{Q} = \{\mathbf{q}_{n,k} \; \forall n, k\}$, and $\Theta = \{\theta_{n,k}[m] \; \forall n, k, m\}$. Constraint (19b) denotes the value range for each aerial IRS reflection element. Constraint (4) indicates the set of the distance constraints due to the maximum flight speed $v_{\max}$. Constraints (9a) and (9b) represent the maximum transmit power and total energy limit, respectively. Constraint (12) ensures the communication QoS for each device. Constraint (18) is the requirement of PAoI.

The coupling of optimization variables causes the constraints (9b) and (12) to be nonconvex and leads to high complexity for the algorithm design. Thus, Problem (P1) is nonconvex and cannot be solved directly by off-the-shelf convex solvers [41]. Although it is difficult to obtain the globally optimal solution, we can solve Problem (P1) approximately by problem decomposition to obtain a near-optimal solution. The technical challenge for solving Problem (P1) lies in the decoupling of optimization variables. It is known that the allocation of the service time determines the evolution of AoI. We observe that the transmit power of devices, aerial IRS deployment, and phase shift jointly determine the data uploading time by affecting the channel quality separately. It is reasonable to separate each variable into a separate group, but the existence of $E_{\max}$ couples the transmit power of devices and data uploading time together. Thus, the optimization variables can be divided into three blocks, i.e., $\{\mathbf{P}, \mathbf{T}\}$, $\mathbf{Q}$, and Θ. We can obtain a near-optimal solution by alternately optimizing each variable block to minimize the objective function.

IV. PROPOSED SOLUTION

In this section, we develop an iterative algorithm based on the BCD method by optimizing the variables in each block alternately with the variables in other blocks fixed. Specifically, we first optimize the transmit power and service time $\{\mathbf{P}, \mathbf{T}\}$ for the given aerial IRS deployment and phase-shift matrix. Then, for the given aerial IRS fight time, data uploading time, transmit power, and aerial IRS phase-shift matrix, we optimize deployment $\mathbf{Q}$. Afterward, for the given aerial IRS deployment, device transmit power, and time allocations, we optimize the phase-shift matrix Θ. The above three steps are repeated until the value of the objective function converges.

A. Transmit Power and Time Optimization

With any given feasible deployment and the phase shift of the aerial IRS, the optimization problem of transmit power and service time $\{\mathbf{P}, \mathbf{T}\}$ can be given by

$$(\text{P2}) \quad \min_{\mathbf{P}, \mathbf{T}} \; \text{AO} \qquad (20)$$
$$\text{s.t.} \quad (4), (9a), (9b), (12), (18).$$

Remark 1: Note that the constraint (12) must hold with equality at the optimal solution of Problem (P2), otherwise the objective function can be decreased by either reducing the data uploading time or increasing the transmit power. For any given feasible deployment and phase shift of the aerial IRS, we can obtain the minimum value of the data uploading time by setting the transmit power as high as possible for minimizing the objective function. When the total energy for each

device is large enough, the device can always upload data at the maximum transmit power $p_{n,k} = P_{\max} \; \forall n \in \mathcal{N}, k \in \mathcal{K}$. The optimal value of AO in Problem (P2) is thus achieved. However, since each device needs to upload N status packets under a limited energy budget $E_{\max}$, it is essential to verify the feasibility of Problem (P2) before solving it.

To minimize the objective function at each iteration, we transform the feasibility check of Problem (P2) into an optimization problem with an explicit objective. By increasing the flight time to large enough, the trajectory constraints (4a)-(4c) must be feasible. Constraints (4d) and (18) are also feasible by setting $T_{\max}$ and A_{th} large enough. Thereby, we need to check the conflict between the total energy budget and data size. To this end, we introduce an auxiliary variable $e_{n,k}$, where $e_{n,k} = T_{n,k,2} p_{n,k}$. The feasibility of Problem (P2) can be checked by considering the following problem, i.e.,

$$(\text{P2a}) \quad \min_{\{T_{n,k,2}, \; e_{n,k}\}} \; \text{AO} \qquad (21a)$$
$$\text{s.t.} \quad e_{n,k} \geq 0 \qquad (21b)$$
$$\sum_{n=1}^{N} e_{n,k} \leq E_{\max} \qquad (21c)$$
$$BT_{n,k,2} \log_2 \left(1 + \frac{e_{n,k}|\boldsymbol{H}_{n,k}|^2}{T_{n,k,2}\sigma^2} \right) \geq D_s \qquad (21d)$$

for all $n \in \mathcal{N}, k \in \mathcal{K}$. Recall that the function $f(x) = x \log(1 + [a/x])$ with $x \geq 0$ is strictly increasing in x, and $f(x)$ approaches to a when x increases to infinity, i.e., $\lim_{x \to \infty} f(x) = a$. Without loss of feasibility, we can readily observe that the inequality in (21d) holds with equality at the optimal solution. Therefore, for the kth device, Problem (P2) is feasible if and only if $E_{\max}$ satisfies the following inequality:

$$\bar{E}_k \triangleq \sum_{n=1}^{N} \frac{\ln 2 D_s \sigma^2}{B|\boldsymbol{H}_{n,k}|^2} \leq E_{\max} \; \forall k \in \mathcal{K}. \qquad (22)$$

Based on the feasibility analysis, we proceed into the algorithm design for solving Problem (P2). By introducing the auxiliary variable $e_{n,k}$, the nonconvex constraint (12) can be rewritten as (21d) which is in the form of perspective function of $\log_2(1 + x)$. Thus, (21d) is a convex constraint. By replacing the nonconvex constraints (9b) and (12) with convex (21c) and (21d), respectively, we obtain

$$(\text{P2b}) \quad \min_{\{e_{n,k}, T_{n,k,1}, T_{n,k,2}\}} \; \text{AO} \qquad (23a)$$
$$\text{s.t.} \quad e_{n,k} \leq P_{\max} T_{n,k,2} \; \forall n \in \mathcal{N}, k \in \mathcal{K} \qquad (23b)$$
$$(4), (18), (21c), (21d).$$

Problem (P2b) is convex and can be solved efficiently by the off-the-shelf convex optimization solvers, e.g., CVX [41]. The details of the proposed iterative algorithm for solving Problem (P2) are shown in Algorithm 1. As long as Problem (P2) is guaranteed to be feasible, the objective function is monotonically nonincreasing after each iteration and lower bounded by zero. Therefore, Problem (P2) can be guaranteed to converge to a stationary point.

Algorithm 1 Iterative Algorithm for Solving Problem (P2)

Input: $B, K, M, P_{\max}, E_{\max}, i = 0, \epsilon > 0$.

1: Initialize $\{\mathbf{q}_{n,k}, \theta_{n,k}[m], \forall n, k\}$;
2: Calculate $\bar{E}_k = \sum_{n=1}^{N} \frac{\ln 2 D_s \sigma^2}{B|H_{n,k}|^2}, \forall k$;
3: **if** $E_{\max} < \bar{E}_k$ **then**
4:     (P2) infeasible, and break;
5: **else**
6:     Introduce $e_{n,k} = T_{n,k,2}p_{n,k}, \forall n, k$;
7:     **repeat**
8:         Set $i = i + 1$;
9:         Obtain $\{\text{AO}^{(i)}, T_{n,k,1}^{(i)}, T_{n,k,2}^{(i)}, e_{n,k}^{(i)}, \forall n, k\}$ by solving Problem (P2b);
10:     **until** $\frac{|\text{AO}^{(i)} - \text{AO}^{(i-1)}|}{\text{AO}^{(i-1)}} \leq \epsilon$;
11:     Calculate $\{p_{n,k}^* = \frac{e_{n,k}}{T_{n,k,2}}, \forall n, k\}$.
12: **end if**

Output: $\{\text{AO}^*, T_{n,k,1}^*, T_{n,k,2}^*, p_{n,k}^*, \forall n, k\}$.

B. Aerial IRS Phase-Shift Design

Given the feasible data uploading time and transmit power of devices, aerial IRS flight time, and deployment positions, Problem (P1) becomes an optimization problem on the phase-shift design of the aerial IRS. Optimizing the phase-shift matrix allows the signals from different paths to be combined coherently at BS. To minimize the average AoI observed at the BS, the achievable communication throughput should be maximized to satisfy constraint (12). Since the feasible variables $\{T_{n,k,1}, T_{n,k,2}, p_{n,k}, \mathbf{q}_{n,k} \, \forall n, k\}$ have been given, the phase-shift design problem is to maximize the channel power gain, which can be written as follows:

$$(\text{P3}) \quad \max_{\Theta} \, |H_{n,k}|^2 \tag{24}$$
$$\text{s.t.} \quad (19b), \, (12).$$

The channel gain $H_{n,k}$ is complex. Given the feasible $\{T_{n,k,2}, p_{n,k}, \mathbf{q}_{n,k} \, \forall n, k\}$ that can satisfy constraint (12), our goal is to find the feasible phase shift $\{\theta_{n,k} \, \forall n, k\}$ that can meet the requirement of constraint (19b) and maximize $|\sum_{m=1}^{M} e^{j(\theta_{n,k}[m] + \psi_{n,k,m} - \varphi_{n,k,m})}|$. Through numerical analysis, we can obtain the optimal phase shift for each aerial IRS element according to Lemma 1.

Lemma 1: For the optimization of Problem (P3), the maximum value of the objective function can be achieved when the phase shift of each element satisfies $\theta_{n,k}[m] = \varphi_{n,k,m} - \psi_{n,k,m}$, for all $n \in \mathcal{N}, k \in \mathcal{K}, m \in \mathcal{M}$.

Proof: Applying the triangle inequality for the array gain of the aerial IRS, we can obtain the inequality as follows:

$$\left| \sum_{m=1}^{M} e^{j(\theta_{n,k}[m] + \psi_{n,k,m} - \varphi_{n,k,m})} \right|$$
$$\leq \left| e^{j(\theta_{n,k}[1] + \psi_{n,k,1} - \varphi_{n,k,1})} \right| + \cdots + \left| e^{j(\theta_{n,k}[m] + \psi_{n,k,m} - \varphi_{n,k,m})} \right|$$
$$+ \cdots + \left| e^{j(\theta_{n,k}[M] + \psi_{n,k,M} - \varphi_{n,k,M})} \right| = M \tag{25}$$

where the equality holds with $\theta_{n,k}[m] = \varphi_{n,k,m} - \psi_{n,k,m}$ [37], [42], for all $n \in \mathcal{N}, k \in \mathcal{K}, m \in \mathcal{M}$.

C. Aerial IRS Deployment Optimization

Given the feasible phase shift and flight time of aerial IRS and transmit power of devices, Problem (P1) is an optimization problem for optimizing the aerial IRS deployment positions $\{\mathbf{q}_{n,k} \, \forall n, k\}$. To guarantee that AO can decrease in the next iteration, our goal in this section is to find the feasible $\mathbf{Q}$ that can maximize the channel power gains. For a fixed-size status packet, increasing $|H_{n,k}|^2$ indicates a decrease in data uploading time. Thus, the objective function value of Problem (P1) is guaranteed to decrease. The optimization of aerial IRS deployment positions can be solved by solving

$$(\text{P4}) \quad \max_{\mathbf{Q}} \, |H_{n,k}|^2 \tag{26}$$
$$\text{s.t.} \quad (4), \, (12).$$

Problem (P4) is a nonconvex problem that cannot be solved directly. The azimuth angles and the elevation steering angles in $\mathbf{h}_{n,k}$ depend on the aerial IRS position $\mathbf{q}_{n,k}$, which makes the optimization of Problem (P4) intractable. In the process of algorithm design, inspired by [35], angles $\{\phi_{n,k}^r, \eta_{n,k}^r, \phi_{n,k}^t, \eta_{n,k}^t \, \forall n, k\}$ in the current iteration can be approximated by the angles obtained in the previous iteration for reducing the difficulty of handling nonconvex constraint (12). This approximation is reasonable as long as the position adjustment range of aerial IRS in adjacent iterations is limited [43]. Otherwise, these angles cannot be considered unchanged. Thus, we introduce a constraint to limit the maximum displacement of the aerial IRS between adjacent iterations of optimizing Problem (P4), i.e.,

$$\left\| \mathbf{q}_{n,k} - \mathbf{q}_{n,k}^{(i)} \right\| \leq \delta_{\max} \quad \forall n \in \mathcal{N}, k \in \mathcal{K} \tag{27}$$

where $\mathbf{q}_{n,k}^{(i)}$ denotes the aerial IRS position in the ith iteration of deployment optimization, and $\delta_{\max}$ represents the maximum allowed displacement of aerial IRS after each iteration. The parameter $\delta_{\max}$ is given by $\delta \leq h\varepsilon_{\max}$, where $\varepsilon_{\max}$ represents the accuracy threshold [44]. It is observed that a relatively small value $\varepsilon_{\max}$ can guarantee the accuracy of the approximation, but it reduces the effectiveness of deployment optimization and increases computational complexity for convergence. Thus, the choice of $\varepsilon_{\max}$ needs to balance the approximation accuracy and computational complexity. In addition, this approximation in the current iteration can take advantage of the optimal phase-shift design in the previous iteration according to Lemma 1.

Afterward, we first do a simple transformation to the nonconvex constraint (12), such that

$$|H_{n,k}|^2 = \frac{|a_{n,k}|^2}{d_{n,k,1}^\alpha d_{n,k,2}^\alpha} \geq b_{n,k} \quad \forall n \in \mathcal{N}, k \in \mathcal{K} \tag{28}$$

where $a_{n,k} = \rho \beta^2 \sum_{m=1}^{M} e^{j(\theta_{n,k}[m] + \psi_{n,k,m} - \varphi_{n,k,m})}$, and $b_{n,k} = ([(2^{(D_s/BT_{n,k,2})} - 1)\sigma^2]/p_{n,k})$. Then, we introduce auxiliary variables $x_{n,k,1}$ and $x_{n,k,2}$, which need to satisfy

$$\|\mathbf{q}_{n,k} - \mathbf{s}_k\|_2^2 + h^2 \leq x_{n,k,1} \quad \forall n \in \mathcal{N}, k \in \mathcal{K} \tag{29a}$$
$$\|\mathbf{q}_{n,k} - \mathbf{s}_0\|_2^2 + h^2 \leq x_{n,k,2} \quad \forall n \in \mathcal{N}, k \in \mathcal{K}. \tag{29b}$$

Algorithm 2 SCA-Based Algorithm for Solving Problem (P4)

Input: $B, K, M, P_{\max}, i = 0, \epsilon > 0$.

1: Initialize $\{T_{n,k,2}, p_{n,k}, \theta_{n,k}[m], \mathbf{q}_{n,k}^{(0)}, \forall n, k, m\}$;
2: Calculate $\{\bar{x}_{n,k,1}, \bar{x}_{n,k,2}, \forall n, k\}$ according
   to $\{\mathbf{q}_{n,k}^{(0)}, \forall n, k\}$;
3: **repeat**
4:     Set iteration index $i = i + 1$;
5:     Substitute $\{\bar{x}_{n,k,1}, \bar{x}_{n,k,2}, \forall n, k\}$ into Eq. (31);
6:     Obtain $\{\mathrm{X}^{(i)}, \mathbf{q}_{n,k}^{(i)}, x_{n,k,1}^{(i)}, x_{n,k,2}^{(i)}, \forall n, k\}$ by
       solving Problem (P4a);
7:     Update $\bar{x}_{n,k,1} = x_{n,k,1}^{(i)}, \bar{x}_{n,k,2} = x_{n,k,2}^{(i)}$ for all n, k;
8: **until** $\frac{|\mathrm{X}^{(i)} - \mathrm{X}^{(i-1)}|}{\mathrm{X}^{(i-1)}} \le \epsilon$.

Output: $\{\mathbf{q}_{n,k}^*, \forall n, k\}$.

Since $f(x) = x^{(2/\alpha)}$ is a monotonically increasing function, we can rewrite (28) as

$$x_{n,k,1} x_{n,k,2} \le c_{n,k}^{\frac{2}{\alpha}} \quad \forall n \in \mathcal{N}, k \in \mathcal{K} \tag{30}$$

where $c_{n,k} = [(|a_{n,k}|^2)/b_{n,k}]$. We deal with the nonconvex constraint by applying SCA technique [45]. We prove that the function $f(x, y) = xy$ is concave about $x > 0$ and $y > 0$ by its second-order condition. Thus, the left-hand side (LHS) of (30) can be approximated by its first-order Taylor approximation as an upper bound

$$\bar{x}_{n,k,1} \bar{x}_{n,k,2} + \bar{x}_{n,k,2}(x_{n,k,1} - \bar{x}_{n,k,1})$$
$$+ \bar{x}_{n,k,1}(x_{n,k,2} - \bar{x}_{n,k,2}) \le c_{n,k}^{\frac{2}{\alpha}} \quad \forall n \in \mathcal{N}, k \in \mathcal{K}. \tag{31}$$

For the objective function $|\boldsymbol{H}_{n,k}|^2$, we rewrite it as $|\boldsymbol{H}_{n,k}|^2 \ge [(|a_{n,k}|^2)/((x_{n,k,1} x_{n,k,2})^{\alpha/2})]$. It is observed that maximizing $|\boldsymbol{H}_{n,k}|^2$ can be achieved by minimizing $x_{n,k,1} x_{n,k,2}$. Thus, we replace $x_{n,k,1} x_{n,k,2}$ by one of its upper bounds, as shown in the LHS of (31), we denote it by X for the sake of brevity. At last, Problem (P4) is approximated by a series of convex problems, where

$$(\text{P4a}) \quad \min_{\{\mathbf{q}_{n,k}, \, x_{n,k,1}, \, x_{n,k,2}\}} \mathrm{X} \tag{32}$$
$$\text{s.t.} \quad (4), (27), (29), (31).$$

Problem (P4a) is a convex problem and can be solved iteratively by the existing convex optimization solvers, e.g., CVX [41], through interior-point methods. The proposed SCA-based algorithm for solving Problem (P4) is shown in Algorithm 2. The objective function of Problem (P4a) is monotonically nonincreasing after each iteration, and it is lower bounded by zero. Thus, a stationary point can be obtained by iteratively solving Problem (P4a).

D. Convergence Analysis

The overall BCD-based algorithm for solving Problem (P1) is summarized in Algorithm 3. It is worth noting that the convergence analysis for the classical BCD algorithm cannot be directly applied in this article. This is because the subproblem

---

Algorithm 3 BCD-Based Algorithm for Solving Problem (P1)

Input: $B, K, M, P_{\max}, E_{\max}, i = 0, \epsilon > 0$.

1: Initialize the feasible aerial IRS deployment and phase
   shift $\{\mathbf{q}_{n,k}^{(0)}, \theta_{n,k}^{(0)}, \forall n, k\}$;
2: Set $\{\bar{\mathbf{q}}_{n,k} = \mathbf{q}_{n,k}^{(0)}, \bar{\theta}_{n,k} = \theta_{n,k}^{(0)}, \forall n, k\}$;
3: **repeat**
4:     Set $i = i + 1$;
5:     Given $\{\bar{\mathbf{q}}_{n,k}, \bar{\theta}_{n,k}, \forall n, k\}$, update $\{\mathrm{AO}^{(i)}, p_{n,k}^{(i)}, T_{n,k,1}^{(i)},$
       $T_{n,k,2}^{(i)}, \forall n, k\}$ by solving (P2) via Algorithm 1;
6:     Given $\{p_{n,k}^{(i)}, T_{n,k,1}^{(i)}, T_{n,k,2}^{(i)}, \forall n, k\}$, update
       $\{\mathbf{q}_{n,k}^{(i)}, \forall n, k\}$ by solving (P4) via Algorithm 2;
7:     Given $\{\mathbf{q}_{n,k}^{(i)}, \forall n, k\}$, calculate $\{\theta_{n,k}^{(i)}, \forall n, k\}$ according
       to Lemma 1;
8:     Update $\bar{\mathbf{q}}_{n,k} = \mathbf{q}_{n,k}^{(i)}, \bar{\theta}_{n,k} = \theta_{n,k}^{(i)}, \forall n, k$;
9: **until** $\frac{|\mathrm{AO}^{(i)} - \mathrm{AO}^{(i-1)}|}{\mathrm{AO}^{(i-1)}} \le \epsilon$.

Output: $\{\mathrm{AO}^*, p_{n,k}^*, T_{n,k,1}^*, T_{n,k,2}^*, \theta_{n,k}^*, \mathbf{q}_{n,k}^*, \forall n, k\}$.

---

for optimizing variables in each block via the BCD method is required to be solved exactly with optimality for ensuring convergence [44]. Thus, we need to prove the convergence of Algorithm 3 based on the solving process of Problem (P1). First, for given $\mathbf{Q}^{(i)}$ and $\Theta^{(i)}$ in step 5 of Algorithm 3, the optimal solution of Problem (P2) can be obtained. Thus, we have

$$\mathrm{AO}\Big(\mathbf{P}^{(i+1)}, \mathbf{T}^{(i+1)}, \mathbf{Q}^{(i)}, \Theta^{(i)}\Big) \le \mathrm{AO}\Big(\mathbf{P}^{(i)}, \mathbf{T}^{(i)}, \mathbf{Q}^{(i)}, \Theta^{(i)}\Big). \tag{33}$$

Second, for given $\mathbf{P}^{(i+1)}$ and $\mathbf{T}^{(i+1)}$ in step 6 of Algorithm 3, $\mathrm{X}^{(i)}$ follows that:

$$\mathrm{X}^{(i)}\Big(\mathbf{P}^{(i+1)}, \mathbf{T}^{(i+1)}, \mathbf{Q}^{(i)}, \Theta^{(i)}\Big)$$
$$\overset{(a)}{=} \mathrm{X}^{(i)}\Big(\mathbf{P}^{(i+1)}, \mathbf{T}^{(i+1)}, \mathbf{Q}^{(i)}, \Theta^{(i)}\Big) \tag{34a}$$
$$\overset{(b)}{\ge} \mathrm{X}^{(i)}\Big(\mathbf{P}^{(i+1)}, \mathbf{T}^{(i+1)}, \mathbf{Q}^{(i+1)}, \Theta^{(i)}\Big) \tag{34b}$$
$$\overset{(c)}{\ge} \mathrm{X}^{(i)}\Big(\mathbf{P}^{(i+1)}, \mathbf{T}^{(i+1)}, \mathbf{Q}^{(i+1)}, \Theta^{(i)}\Big) \tag{34c}$$

where (a) holds since the first-order Taylor expansions in (31) is tight at the given local points; (b) holds since Problem (P4a) is solved optimally with $\mathbf{Q}^{(i+1)}$; and (c) holds since the optimal objective value of Problem (P4a) is an upper bound at $\mathbf{Q}^{(i+1)}$. Equation (34) indicates that Problem (P4a) is monotonically nonincreasing as the iteration number increases. Thus, the original objective function value AO follows that:

$$\mathrm{AO}^{(i)}\Big(\mathbf{P}^{(i+1)}, \mathbf{T}^{(i+1)}, \mathbf{Q}^{(i)}, \Theta^{(i)}\Big) \tag{35a}$$
$$\ge \mathrm{AO}^{(i)}\Big(\mathbf{P}^{(i+1)}, \mathbf{T}^{(i+1)}, \mathbf{Q}^{(i+1)}, \Theta^{(i)}\Big). \tag{35b}$$

Third, for given $\mathbf{P}^{(i+1)}$, $\mathbf{T}^{(i+1)}$ and $\mathbf{Q}^{(i+1)}$ in step 7 of Algorithm 3, it follows that:

$$\mathrm{AO}^{(i)}\Big(\mathbf{P}^{(i+1)}, \mathbf{T}^{(i+1)}, \mathbf{Q}^{(i+1)}, \Theta^{(i)}\Big)$$
$$\ge \mathrm{AO}^{(i)}\Big(\mathbf{P}^{(i+1)}, \mathbf{T}^{(i+1)}, \mathbf{Q}^{(i+1)}, \Theta^{(i+1)}\Big). \tag{36}$$

This shows that the objective function value of Problem (P1) can be guaranteed to be nonincreasing according to the calculation of $\Theta^{(i+1)}$ via Lemma 1. Based on the above analysis, i.e., (33)–(36), we obtain

$$\mathrm{AO}^{(i)}\left(\mathbf{P}^{(i)}, \mathbf{T}^{(i)}, \mathbf{Q}^{(i)}, \Theta^{(i)}\right)$$
$$\geq \mathrm{AO}^{(i)}\left(\mathbf{P}^{(i+1)}, \mathbf{T}^{(i+1)}, \mathbf{Q}^{(i+1)}, \Theta^{(i+1)}\right) \quad (37)$$

which confirms that the objective function value of Problem (P1) is monotonically nonincreasing after each iteration in Algorithm 3. Meanwhile, the objective function value of Problem (P1) is also lower bounded by zero, the proposed BCD-based algorithm thus can be guaranteed to converge to a stationary point. Moreover, simulation results show that the proposed algorithm can converge quickly in wireless networks with a medium number of IoT devices.

E. Computational Complexity

Since there are only convex subproblems that need to be solved in each iteration of Algorithm 3, the corresponding computational complexity is polynomial. The total computational complexity of the proposed algorithm is analyzed as follows: The computational complexity of applying Algorithm 1 is determined by the number of iterations and the computational complexity for solving Problem (P2) in each iteration [25]. The computational complexity in each iteration is $\mathcal{O}((3NK)^3)$ since there are $3NK$ variables that need to be updated in each iteration. Thus, the total computational complexity of Algorithm 1 is $\mathcal{O}(I_1(3NK)^3)$, where I_1 represents the required number of iterations for achieving convergence. Similarly, the computational complexity of applying Algorithm 2 is $\mathcal{O}(I_2(3NK)^3)$. Although it is difficult to acquire the exact value of iteration number $\{I_1, I_2\}$, multiple simulation results demonstrate that both Algorithms 1 and 2 converge within several iterations under a given precision. Therefore, the total computational complexity for approximately solving (P₁) is $\mathcal{O}(I_0(I_1 + I_2)(3NK)^3)$, where I_0 is the number of iterations needed for convergence of the proposed algorithm. Considering an offline joint optimization, the computational complexity of the proposed algorithm is acceptable under the given available computing power.

Remark 2: Based on Remark 1, as long as the total energy budget $E_{\max}$ for each device is large enough, e.g., devices can be charged regularly, the device can always upload the status packet at $P_{\max}$. In this case, there is no need to optimize transmit power, the total computational complexity for approximately solving (P₁) is reduced to $\mathcal{O}(I_0(I_1(2NK)^3 + I_2(3NK)^3))$.

V. SIMULATION RESULTS

We consider a network scenario in which an aerial IRS assists K IoT devices distributed in a square area with a side length of 100 m. Since K devices are scattered over a relatively concentrated area, the visiting sequence is predefined according to the nearest neighbor criterion, i.e., the aerial IRS always chooses the device closest to its current position. For easy setup, we set the status packet size to be the same for

TABLE I
SIMULATION PARAMETERS

Parameters	Values	Parameters	Values
N	5	K	5
M	16	B	1 KHz
h	100 m	$\mathbf{q}_{\mathrm{s}}$	$[0, 0]^T$
$\boldsymbol{s}_0$	$[250, 250]^T$	$\mathbf{q}_{\mathrm{e}}$	$[500, 500]^T$
$P_{\max}$	20 dBm	$E_{\max}$	50 J
$T_{\max}$	150 s	$v_{\max}$	20 m/s
ρ	10 dBm	α	2.3
σ^2	-110 dBm	κ	10 dB
$\delta_{\max}$	50 m	d	$\lambda/2$
A_{th}	50 s	D_s	1 Kbits

all devices. Simulation results are presented in this section to show the impact of the different parameter settings on AoI and verify the effectiveness of the proposed BCD-based algorithm.

A. Simulation Setup

Unless stated otherwise, parameter settings [21] are shown in Table I. For any given feasible aerial IRS deployment, a feasible IRS phase-shift matrix is initialized according to Lemma 1. Moreover, the proposed solution (AIRS) in this article is compared to the following benchmarks.

1) *FIRS:* We provide three deployment schemes with the fixed aerial IRS positions for comparison. Specifically, the first deployment scheme (FIRS-1) is that the aerial IRS is deployed directly above the device being served, i.e., $\{\mathbf{q}_{n,k} = \boldsymbol{s}_k \ \forall n, k\}$. The second (FIRS-2) is deploying the aerial IRS in the middle of each device and BS, i.e., $\{\mathbf{q}_{n,k} = [(\boldsymbol{s}_k + \boldsymbol{s}_0)/2] \ \forall n, k\}$. The third (FIRS-3) is that we deploy the aerial IRS evenly in a straight line between starting position $\mathbf{q}_{\mathrm{s}}$ and end position $\mathbf{q}_{\mathrm{e}}$, i.e., $x_{n,k} = x_{\mathrm{s}} + ((n-1)K + k)\triangle x$ and $y_{n,k} = y_{\mathrm{s}} + ((n-1)K + k) \triangle y$, where $\triangle x = [(x_{\mathrm{e}} - x_{\mathrm{s}})/N(K+1)]$, $\triangle y = ([y_{\mathrm{e}} - y_{\mathrm{s}}]/[N(K+1)])$. For FIRS, there are only the transmit power, data uploading time, aerial IRS flight time, and aerial IRS phase shift that needs to be optimized. The corresponding algorithm design can refer to the proposed algorithm in this article which is omitted here for brevity.

2) *AcRelay:* In this benchmark scheme, one UAV is deployed as an AcRelay in our considered scenario to assist in collecting the status packet from each device and then forwarding it to the BS [30], [31]. This benchmark scheme placed the UAV at the optimized deployment positions of the aerial IRS and ignored the power attenuation from the device to the UAV, i.e., setting the UAV transmit power as $P_{\max}$, for ensuring comparative fairness. The channel model and visiting sequence are consistent with this work.

B. Convergence of Proposed Algorithm

We present the convergence behavior of the proposed algorithm during each iteration in Fig. 3. Simulation results
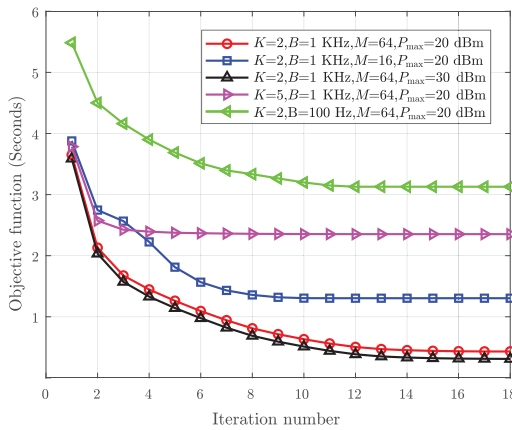
Fig. 3. Convergence of the proposed algorithm with various simulation parameter settings.

indicate that the relative convergence accuracy can be guaranteed to be lower than 10^{-3} within several iterations for different parameter setups. We can easily find that increasing B, M, and P_{max} can reduce the value of the objective function, but they have less impact on the convergence of the proposed algorithm. It is also observed that increasing K will increase the objective function but speed up the convergence rate. This is mainly because the more devices in the distribution area, the more efficient it is in quickly determining the deployment area of the aerial IRS.

C. Aerial IRS Deployment

In Fig. 4(a), under the default parameter settings, the optimal aerial IRS deployment with $K = 10$ for the proposed algorithm in a time frame is presented. As we can see, the positions where the aerial IRS is deployed for different devices are close. This is because devices are located in a relatively concentrated area, this deployment approach can save the UAV flight time when serving adjacent devices. In different time frames, the deployment positions of the aerial IRS for the same device are almost the same. To dig up more information about the deployment, we give a general case as shown in Fig. 4(b).

We present the optimized aerial IRS trajectory with $K = 3$ as an example to show how the aerial IRS assists in communication over multiple time frames in Fig. 4(b). As shown in this figure, the aerial IRS departs from $\mathbf{q}_s$ and flies directly to position 1, and then assists device s_1 to upload the status packet to the BS. Then, the aerial IRS assists the uploading tasks of s_2 and s_3 in position 2 and position 3, respectively. Until the device s_3 completes the data uploading, which means the end of the first time frame. Then, the aerial IRS moves directly to position 1 for starting the second time frame. The optimized aerial IRS deployment positions form a triangle to reduce the flight time between adjacent time frames. Until N time frames are completed, the aerial IRS returns to $\mathbf{q}_e$.

D. Impact of Parameters on AoI

In Fig. 5, we illustrate the AoI evolution over time for two devices under different parameter setups. As shown in Fig. 5,

it is observed that the PAoI values for two devices are all less than the upper limit A_{th}. For the observation at any time, the AoI of the status packet generated by the first device is always older than that of the second device. This is caused by the difference in the visiting priority. But it is not always bad for the first-served device, as we can see, the PAoI of the first device is much smaller than that of the second device. Therefore, in the practical system design, we can specify the visiting priority of devices according to the different AoI-related requirements of the application.

In addition, we observe that increasing B, M, and P_{max} can all help to reduce AO. Furthermore, it is observed that the gap of AoI for different devices observed at any time can be reduced by increasing B, M, and P_{max}, and so does the gap of PAoI for different devices. This is instructive for applications that require AoI-fairness. In Fig. 5(a), we observe that increasing the bandwidth B by ten times can best reduce the AoI of the status data and ensure the AoI-fairness of the system. However, this approach is not suitable for applications with limited bandwidth resources. We observe from Fig. 5(b) that the performance of reducing AoI by quadrupling the number of IRS elements M is between increasing P_{max} and B. This approach reduces the PAoI difference between two devices to almost zero, which can provide insight for fair design in applications. More performance gains can be achieved by further increasing M, this fact will be presented in Fig. 8. It is observed in Fig. 5(c) that the performance improvement in reducing AoI is relatively limited by increasing the transmit power P_{max} ten times. And this approach is not friendly to energy-constrained devices.

E. Comparison With Benchmarks

It is observed in Fig. 6 that increasing P_{max} and B both have an active impact on the objective function AO, and the impact of the latter is more obvious. It can be seen that AO decays rapidly with P_{max}, especially when $B = 200$ Hz. This means that the impact of transmit power on AO is dominant when the bandwidth is small. However, when P_{max} increases to a certain extent, e.g., 40 dBm or more, AO no longer decreases. This means that AO cannot be reduced indefinitely with P_{max}. When the transmit power is small, $P_{max} = 20$ dBm in our simulation, the impact of bandwidth B on AoI dominates. For example, when P_{max} is fixed as 20 dBm, we change B from 200 Hz to 1.0 KHz, and the objective function goes down by 80%. When B is fixed as 200 Hz, we change P_{max} from 20 to 30 dBm, and the objective function goes down by 68.46%. This reveals that the impact of B on AO is more obvious than P_{max}. This fact has been proved from the comparison between Fig. 5(a) and (c). Furthermore, we observe that optimizing the deployment of the aerial IRS is essential for ensuring the information freshness, and this way has great potential for energy savings. As shown in Fig. 6, although the AO decreases with P_{max} increasing until it reaches a stable value for all schemes, the proposed solution in this article has the best performance on the whole. The benchmark FIRS has the worst performance, and its algorithm performance varies greatly with deployment position. AcRelay and AIRS
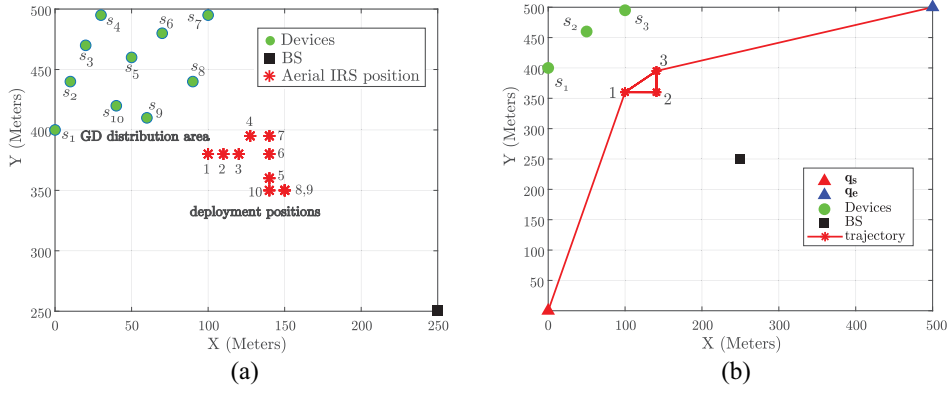
Fig. 4.   Aerial IRS deployment obtained by the proposed algorithm: the index i of the aerial IRS deployment position corresponding to the device s_i. (a) Aerial IRS deployment with $K = 10$. (b) Aerial IRS trajectory with $K = 3$.
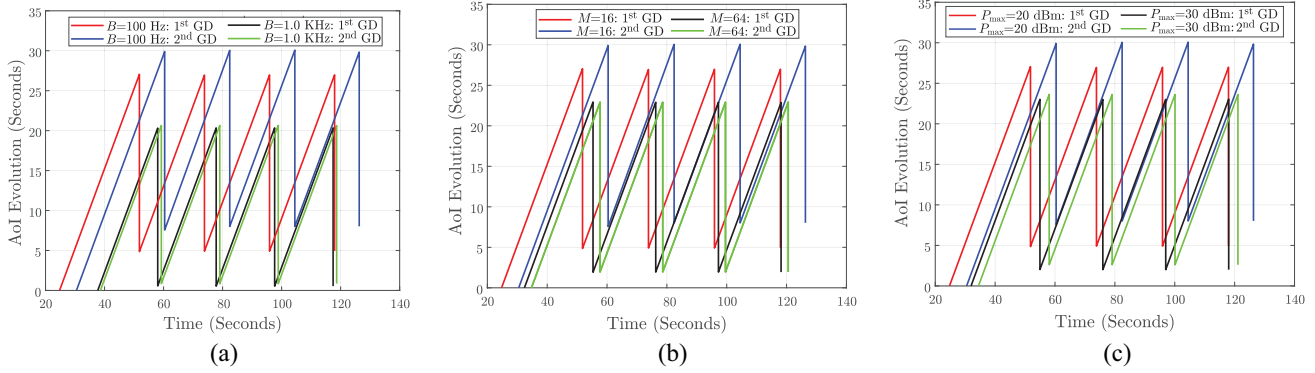
Fig. 5.   AoI evolution over time under different parameter setups. (a) $M = 16$ and $P_{\max} = 20$ dBm. (b) $B = 100$ Hz and $P_{\max} = 20$ dBm. (c) $B = 100$ Hz and $M = 64$.
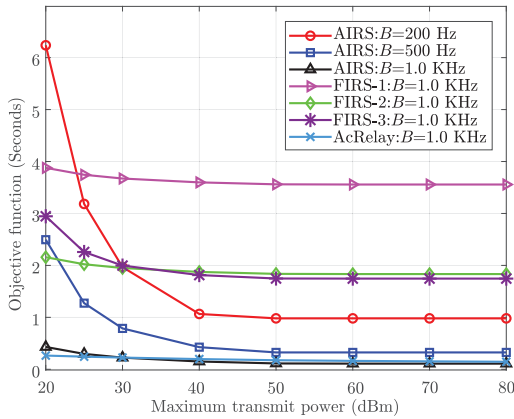
Fig. 6.   Comparison of the proposed solution (AIRS) and benchmark schemes under different values of $P_{\max}$ and B.
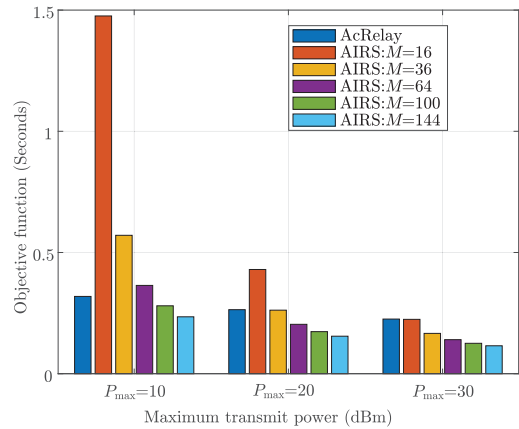
Fig. 7.   Comparison of the passive relay (AIRS) and the AcRelay under different values of $P_{\max}$.

have similar performance, and they have an intersection at $P_{\max} = 30$ dBm.

To further explore the performance gap between AcRelay and AIRS, the comparison of the AcRelay and passive relay under different $P_{\max}$ is shown in Fig. 7. It is observed that the AcRelay performs better than the passive relay when M is small, e.g., 16. Although increasing $P_{\max}$ can narrow the gap between them, however, this method for performance improvement is not efficient since it will increase energy consumption. Interestingly, we observe that increasing M can improve the performance

gain of AIRS. For AIRS, M has more significant impact on AO than $P_{\max}$. Even when $P_{\max}$ is large, e.g., 30 dBm, aerial IRS with $M = 36$ performs better than the AcRelay. Whatever the value of $P_{\max}$ is, increasing the number of IRS elements can bring significant performance gains by improving channel quality. This reveals that the passive relay performs better than the AcRelay not only in improving the information freshness but also in energy saving. For example, when $P_{\max} = 20$ dBm, the objective function value of AcRelay is 70.72% higher than the value of AIRS with $M = 144$.
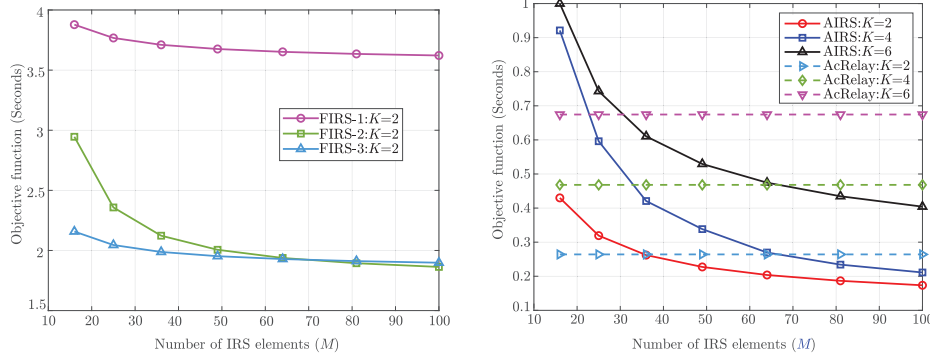
Fig. 8.   Comparison of the proposed solution (AIRS) and benchmarks (FIRS, AcRelay) under different values of M and K.

We present the impact of M and K on the objective function AO under different schemes in Fig. 8. Among these schemes, the proposed solution based on AIRS has the best performance on the whole. It shows that AO increases significantly with the increase in K for all algorithms. AcRelay is not affected by M, but for AIRS and FIRS, the objective function can be well reduced by improving the channel quality, i.e., increasing M. This shows that the deployment position of the aerial IRS has a significant impact on the freshness of information. Optimizing aerial IRS deployment can bring significant performance improvement to the information freshness, especially when M is large, e.g., 100. In addition, we observe that the decline slope gradually decreases with the increase in M for AIRS and FIRS. This indicates that the channel quality cannot be enhanced infinitely, but a larger value of M can reduce the impact of K on AO. For $K = 2$ and 6, increasing M from 16 to 100 results in the objective function declines of 0.26 and 0.60 s, respectively. This means that M has a greater impact on the gain of improving system performance when K is larger. This fact has also been illustrated in Fig. 6.

These results provide more flexible operational options for performance improvements in practical applications. Both the proposed solution and benchmark schemes can improve the quality of the communication in the case of long propagation distance or the existence of blockages, but the proposed aerial IRS is more energy-efficient and has greater operational flexibility and higher performance gains. Although the scale of the reflective panel the UAV carries is limited, the limited improvement of the channel quality also greatly helps to improve the information freshness.

VI. CONCLUSION

In this article, we have investigated an average AoI minimization problem for an aerial IRS-assisted remote IoT to improve the freshness of information. We have proposed a BCD-based iterative algorithm to solve this nonconvex minimization problem with coupled variables. The significance of this work is that the aerial IRS is verified to be energy-efficient and flexible to deploy for improving information freshness. This draws useful insights into deploying the aerial IRSs to enhance the communication quality for supporting time-critical applications. For future work, we will evaluate

the cooperation of multiple distributed aerial IRSs to further improve the information freshness for the networks with massive devices.

REFERENCES

[1] M. Vaezi et al., "Cellular, wide-area, and non-terrestrial IoT: A survey on 5G advances and the road toward 6G," *IEEE Commun. Surveys Tuts.*, vol. 24, no. 2, pp. 1117–1174, 2nd Quart., 2022.

[2] M. Li, J. Gao, L. Zhao, and X. Shen, "Adaptive computing scheduling for edge-assisted autonomous driving," *IEEE Trans. Veh. Technol.*, vol. 70, no. 6, pp. 5318–5331, Jun. 2021.

[3] M. A. Abd-Elmagid, N. Pappas, and H. S. Dhillon, "On the role of age of information in the Internet of Things," *IEEE Commun. Mag.*, vol. 57, no. 12, pp. 72–77, Dec. 2019.

[4] M. Li, C. Chen, H. Wu, X. Guan, and X. Shen, "Age-of-information aware scheduling for edge-assisted industrial wireless networks," *IEEE Trans. Ind. Informat.*, vol. 17, no. 8, pp. 5562–5571, Aug. 2021.

[5] S. Kaul, R. Yates, and M. Gruteser, "Real-time status: How often should one update?" in *Proc. IEEE INFOCOM*, 2012, pp. 2731–2735.

[6] R. D. Yates, Y. Sun, D. R. Brown, S. K. Kaul, E. Modiano, and S. Ulukus, "Age of information: An introduction and survey," *IEEE J. Sel. Areas Commun.*, vol. 39, no. 5, pp. 1183–1210, May 2021.

[7] A. Kosta, N. Pappas, and V. Angelakis, *Age of Information: A New Concept, Metric, and Tool*. Hanover, MA, USA: Now Publ., 2017.

[8] H. S. Dhillon, H. Huang, and H. Viswanathan, "Wide-area wireless communication challenges for the Internet of Things," *IEEE Commun. Mag.*, vol. 55, no. 2, pp. 168–174, Feb. 2017.

[9] H. Zhang, L. Song, and Z. Han, *Unmanned Aerial Vehicle Applications Over Cellular Networks for 5G and Beyond*. Cham, Switzerland: Springer, 2020.

[10] R. Chen, M. Liu, Y. Hui, N. Cheng, and J. Li, "Reconfigurable intelligent surfaces for 6G IoT wireless positioning: A contemporary survey," *IEEE Internet Things J.*, vol. 9, no. 23, pp. 23570–23582, Dec. 2022.

[11] Q. Wu and R. Zhang, "Towards smart and reconfigurable environment: Intelligent reflecting surface aided wireless network," *IEEE Commun. Mag.*, vol. 58, no. 1, pp. 106–112, Jan. 2020.

[12] G. Zhang, C. Shen, B. Ai, and Z. Zhong, "Robust symbol-level precoding and passive beamforming for IRS-aided communications," *IEEE Trans. Wireless Commun.*, vol. 21, no. 7, pp. 5486–5499, Jul. 2022.

[13] H. Lu, Y. Zeng, S. Jin, and R. Zhang, "Aerial intelligent reflecting surface: Joint placement and passive beamforming design with 3D beam flattening," *IEEE Trans. Wireless Commun.*, vol. 20, no. 7, pp. 4128–4143, Jul. 2021.

[14] S. Alfattani et al., "Aerial platforms with reconfigurable smart surfaces for 5G and beyond," *IEEE Commun. Mag.*, vol. 59, no. 1, pp. 96–102, Jan. 2021.

[15] Z. Ma et al., "Modeling and analysis of MIMO multipath channels with aerial intelligent reflecting surface," *IEEE J. Sel. Areas Commun.*, vol. 40, no. 10, pp. 3027–3040, Oct. 2022.

[16] A. Muhammad, M. Elhattab, M. A. Arfaoui, A. Al-Hilo, and C. Assi, "Age of information optimization in a RIS-assisted wireless network," 2021, *arXiv:2103.06405*.

[17] R. Ding, F. Gao, and X. S. Shen, "3D UAV trajectory design and frequency band allocation for energy-efficient and fair communication: A deep reinforcement learning approach," *IEEE Trans. Wireless Commun.*, vol. 19, no. 12, pp. 7796–7809, Dec. 2020.

[18] M. Li, N. Cheng, J. Gao, Y. Wang, L. Zhao, and X. Shen, "Energy-efficient UAV-assisted mobile edge computing: Resource allocation and trajectory optimization," *IEEE Trans. Veh. Technol.*, vol. 69, no. 3, pp. 3424–3438, Mar. 2020.

[19] M. Fu, Y. Zhou, Y. Shi, C. Jiang, and W. Zhang, "UAV-assisted multi-cluster over-the-air computation," *IEEE Trans. Wireless Commun.*, early access, Dec. 14, 2022, doi: 10.1109/TWC.2022.3227768.

[20] "Enhanced LTE support for aerial vehicles," 3GPP, Sophia Antipolis, France, 3GPP Rep. TR 36.777, 2018.

[21] M. Samir, M. Elhattab, C. Assi, S. Sharafeddine, and A. Ghrayeb, "Optimizing age of information through aerial reconfigurable intelligent surfaces: A deep reinforcement learning approach," *IEEE Trans. Veh. Technol.*, vol. 70, no. 4, pp. 3978–3983, Apr. 2021.

[22] X. Shen, J. Gao, W. Wu, M. Li, C. Zhou, and W. Zhuang, "Holistic network virtualization and pervasive network intelligence for 6G," *IEEE Commun. Surveys Tuts.*, vol. 24, no. 1, pp. 1–30, 1st Quart., 2022.

[23] X. Shen et al., "AI-assisted network-slicing based next-generation wireless networks," *IEEE Open J. Veh. Technol.*, vol. 1, pp. 45–66, 2020.

[24] Q. Wu et al., "A comprehensive overview on 5G-and-beyond networks with UAVs: From communications to sensing and intelligence," *IEEE J. Sel. Areas Commun.*, vol. 39, no. 10, pp. 2912–2945, Oct. 2021.

[25] S. Boyd and L. Vandenberghe, *Convex Optimization*. Cambridge, MA, USA: MIT Press, 2004.

[26] J. Gong, T.-H. Chang, C. Shen, and X. Chen, "Flight time minimization of UAV for data collection over wireless sensor networks," *IEEE J. Sel. Area Commun.*, vol. 36, no. 9, pp. 1942–1954, Sep. 2018.

[27] C. Zhan and Y. Zeng, "Completion time minimization for multi-UAV-enabled data collection," *IEEE Trans. Wireless Commun.*, vol. 18, no. 10, pp. 4859–4872, Oct. 2019.

[28] C. Shen, T.-H. Chang, J. Gong, Y. Zeng, and R. Zhang, "Multi-UAV interference coordination via joint trajectory and power control," *IEEE Trans. Signal Process.*, vol. 68, pp. 843–858, Jan. 2020, doi: 10.1109/TSP.2020.2967146.

[29] C. Zhou et al., "Deep RL-based trajectory planning for AoI minimization in UAV-assisted IoT," in *Proc. IEEE WCSP*, 2019, pp. 1–6.

[30] M. A. Abd-Elmagid and H. S. Dhillon, "Average peak age-of-information minimization in UAV-assisted IoT networks," *IEEE Trans. Veh. Technol.*, vol. 68, no. 2, pp. 2003–2008, Feb. 2019.

[31] W. Jiang, C. Shen, B. Ai, and H. Li, "Peak age of information minimization for UAV-aided wireless sensing and communications," in *Proc. IEEE ICC Workshops*, 2021, pp. 1–6.

[32] S. Zhang, H. Zhang, Z. Han, H. V. Poor, and L. Song, "Age of information in a cellular Internet of UAVs: Sensing and communication trade-off design," *IEEE Trans. Wireless Commun.*, vol. 19, no. 10, pp. 6578–6592, Oct. 2020.

[33] T. Wu et al., "A novel AI-based framework for AoI-optimal trajectory planning in UAV-assisted wireless sensor networks," *IEEE Trans. Wireless Commun.*, vol. 21, no. 4, pp. 2462–2475, Apr. 2022.

[34] A. Al-Hilo, M. Samir, M. Elhattab, C. Assi, and S. Sharafeddine, "RIS-assisted UAV for timely data collection in IoT networks," *IEEE Syst. J.*, vol. 17, no. 1, pp. 431–442, Mar. 2023.

[35] X. Mu, Y. Liu, L. Guo, J. Lin, and H. V. Poor, "Intelligent reflecting surface enhanced multi-UAV NOMA networks," *IEEE J. Sel. Areas Commun.*, vol. 39, no. 10, pp. 3051–3066, Oct. 2021.

[36] A. Khalili, E. M. Monfared, S. Zargari, M. R. Javan, N. M. Yamchi, and E. A. Jorswieck, "Resource management for transmit power minimization in UAV-assisted RIS HetNets supported by dual connectivity," *IEEE Trans. Wireless Commun.*, vol. 21, no. 3, pp. 1806–1822, Mar. 2022.

[37] W. Lyu, Y. Xiu, S. Yang, P. L. Yeoh, Y. Li, and Z. Zhang, "Weighted sum age of information minimization in wireless networks with aerial IRS," *IEEE Trans. Veh. Technol.*, early access, Nov. 28, 2022, doi: 10.1109/TVT.2022.3223691.

[38] Z. Abdullah, G. Chen, S. Lambotharan, and J. A. Chambers, "A hybrid relay and intelligent reflecting surface network and its ergodic performance analysis," *IEEE Wireless Commun. Lett.*, vol. 9, no. 10, pp. 1653–1657, Oct. 2020.

[39] W. Wu, N. Cheng, N. Zhang, P. Yang, W. Zhuang, and X. Shen, "Fast mmWave beam alignment via correlated bandit learning," *IEEE Trans. Wireless Commun.*, vol. 18, no. 12, pp. 5894–5908, Dec. 2019.

[40] B. Zheng, C. You, and R. Zhang, "Intelligent reflecting surface assisted multi-user OFDMA: Channel estimation and training design," *IEEE Trans. Wireless Commun.*, vol. 19, no. 12, pp. 8315–8329, Dec. 2020.

[41] M. Grant and S. Boyd. "CVX: MATLAB software for disciplined convex programming, version 2.1." Mar. 2014. [Online]. Available: http://cvxr.com/cvx

[42] M. Elhattab, M.-A. Arfaoui, C. Assi, and A. Ghrayeb, "Reconfigurable intelligent surface assisted coordinated multipoint in downlink NOMA networks," *IEEE Commun. Lett.*, vol. 25, no. 2, pp. 632–636, Feb. 2021.

[43] D. Xu, Y. Sun, D. W. K. Ng, and R. Schober, "Multiuser MISO UAV communications in uncertain environments with no-fly zones: Robust trajectory and resource allocation design," *IEEE Trans. Commun.*, vol. 68, no. 5, pp. 3153–3172, May 2020.

[44] Q. Wu, Y. Zeng, and R. Zhang, "Joint trajectory and communication design for multi-UAV enabled wireless networks," *IEEE Trans. Wireless Commun.*, vol. 17, no. 3, pp. 2109–2121, Mar. 2018.

[45] W.-C. Li, T.-H. Chang, and C.-Y. Chi, "Multicell coordinated beamforming with rate outage constraint—Part II: Efficient approximation algorithms," *IEEE Trans. Signal Process.*, vol. 63, no. 11, pp. 2763–2778, Jun. 2015.

Wenwen Jiang (Graduate Student Member, IEEE) received the B.S. degree in communication engineering from Shandong Normal University, Jinan, China, in 2018. She is currently pursuing the Ph.D. degree with the State Key Laboratory of Rail Traffic Control and Safety, Beijing Jiaotong University, Beijing, China.

She is currently a Visiting Ph.D. Student with the University of Waterloo, Waterloo, ON, Canada. Her current research interests include UAV communications, Age of Information, IRS-assisted communications, and mobile-edge computing.

Bo Ai (Fellow, IEEE) received the M.S. and Ph.D. degrees from Xidian University, Xi'an, China, in 2002 and 2004, respectively.

He was with Tsinghua University, Beijing, China, where he was an Excellent Postdoctoral Research Fellow in 2007. He was a Visiting Professor with the Electrical Engineering Department, Stanford University, Stanford, CA, USA, in 2015. He is currently a Full Professor with Beijing Jiaotong University, Beijing, where he is the Dean of the School of Electronic and Information Engineering, and the Deputy Director of the State Key Laboratory of Rail Traffic Control and Safety and the International Joint Research Center. He is one of the directors of Beijing Urban Rail Operation Control System International Science and Technology Cooperation Base, Beijing, and the Backbone Member of the Innovative Engineering based jointly granted by the Chinese Ministry of Education and the State Administration of Foreign Experts Affairs. He is the Research Team Leader of 26 national projects. He holds 26 invention patents. His research interests include the research and applications of channel measurement and channel modeling and dedicated mobile communications for rail traffic systems. He has authored or coauthored eight books and authored over 300 academic research articles in his research area.

Dr. Ai received the Honor of Excellent Postdoctoral Research Fellow from Tsinghua University in 2007. He received the Distinguished Youth Foundation and Excellent Youth Foundation from the National Natural Science Foundation of China, the Qiushi Outstanding Youth Award by the Hong Kong Qiushi Foundation, the New Century Talents by the Chinese Ministry of Education, the Zhan Tianyou Railway Science and Technology Award by the Chinese Ministry of Railways, and the Science and Technology New Star by the Beijing Municipal Science and Technology Commission. He has won some important scientific research prizes. Five papers have been the ESI Highly Cited Paper. He has been notified by the Council of Canadian Academies that based on the Scopus database, and has been listed as one of the top 1% authors in his field all over the world. He has also been feature interviewed by the *Electronics Letters* [Institution of Engineering and Technology (IET)]. He is an IEEE VTS Beijing Chapter Vice Chair and an IEEE BTS Xi' an Chapter Chair. He was a co-chair or a session/track chair of many international conferences. He is an Associate Editor of the IEEE ANTENNAS AND WIRELESS PROPAGATION LETTERS and IEEE TRANSACTIONS ON CONSUMER ELECTRONICS, and an Editorial Committee Member of the *Wireless Personal Communications*. He is the Lead Guest Editor of Special Issues on the IEEE TRANSACTIONS ON VEHICULAR TECHNOLOGY, IEEE ANTENNAS AND PROPAGATIONS LETTERS, and *International Journal on Antennas and Propagations*. He is a Fellow of IET and an IEEE VTS Distinguished Lecturer.
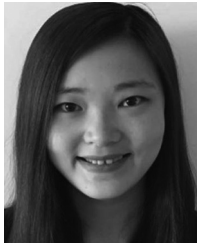
Mushu Li (Member, IEEE) received the M.A.Sc. degree from Toronto Metropolitan University, Canada, in 2017, and the Ph.D. degree in electrical and computer engineering from the University of Waterloo, Waterloo, ON, Canada, in 2021.

She is currently a Postdoctoral Fellow with Toronto Metropolitan University, Toronto, ON, Canada. She was a Postdoctoral Fellow with the University of Waterloo from 2021 to 2022. Her research interests include mobile-edge computing, the system optimization in wireless networks, and machine-learning-assisted network management.

Dr. Li was the recipient of the Natural Science and Engineering Research Council of Canada (NSERC) Postdoctoral Fellowship in 2022, the NSERC Canada Graduate Scholarship in 2018, and the Ontario Graduate Scholarship 2015 and 2016.

Wen Wu (Senior Member, IEEE) received the B.E. degree in information engineering from the South China University of Technology, Guangzhou, China, in 2012, the M.E. degree in electrical engineering from the University of Science and Technology of China, Hefei, China, in 2015, and the Ph.D. degree in electrical and computer engineering from the University of Waterloo, Waterloo, ON, Canada, in 2019.

He worked as a Postdoctoral Fellow with the Department of Electrical and Computer Engineering, University of Waterloo. He is currently an Associate Researcher with the Frontier Research Center, Peng Cheng Laboratory, Shenzhen, China. His research interests include 6G networks, network intelligence, and network virtualization.

Xuemin (Sherman) Shen (Fellow, IEEE) received the Ph.D. degree in electrical engineering from Rutgers University, New Brunswick, NJ, USA, in 1990.

He is a University Professor with the Department of Electrical and Computer Engineering, University of Waterloo, Waterloo, ON, Canada. His research focuses on network resource management, wireless network security, Internet of Things, 5G and beyond, and vehicular networks.

Dr. Shen received the Canadian Award for Telecommunications Research from the Canadian Society of Information Theory in 2021, the R.A. Fessenden Award in 2019 from IEEE, Canada, the Award of Merit from the Federation of Chinese Canadian Professionals (Ontario) in 2019, the James Evans Avant Garde Award in 2018 from the IEEE Vehicular Technology Society, the Joseph LoCicero Award in 2015 and Education Award in 2017 from the IEEE Communications Society, and the Technical Recognition Award from Wireless Communications Technical Committee in 2019 and AHSN Technical Committee in 2013. He has also received the Excellent Graduate Supervision Award in 2006 from the University of Waterloo and the Premier's Research Excellence Award in 2003 from the Province of Ontario, Canada. He served as the Technical Program Committee Chair/Co-Chair for IEEE Globecom'16, IEEE Infocom'14, IEEE VTC'10 Fall, IEEE Globecom'07, and the Chair for the IEEE Communications Society Technical Committee on Wireless Communications. He is the President of the IEEE Communications Society. He was the Vice President for Technical & Educational Activities, Vice President for Publications, Member-at-Large on the Board of Governors. He was/is the Editor-in-Chief of the IEEE INTERNET OF THINGS JOURNAL, *IEEE Network Magazine*, *IET Communications*, and *Peer-to-Peer Networking and Applications*. He is a registered Professional Engineer of Ontario, a Chinese Academy of Engineering Foreign Member, a Distinguished Lecturer of the IEEE Vehicular Technology Society and Communications Society, and a Fellow of the Engineering Institute of Canada, Canadian Academy of Engineering, and Royal Society of Canada.